



RESEARCH ARTICLE

Integrative Cardiovascular Physiology and Pathophysiology

On the assessment of arterial compliance from carotid pressure waveform

 Vasiliki Bikia,¹ Patrick Segers,²  Georgios Rovas,¹ Stamatia Pagoulidou,¹ and Nikolaos Stergiopoulos¹

¹Laboratory of Hemodynamics and Cardiovascular Technology, Institute of Bioengineering, Swiss Federal Institute of Technology, Lausanne, Vaud, Switzerland and ²IBiTech, University of Ghent, Ghent, East Flanders, Belgium

Abstract

In a progressively aging population, it is of utmost importance to develop reliable, noninvasive, and cost-effective tools to estimate biomarkers that can be indicative of cardiovascular risk. Various pathophysiological conditions are associated to changes in the total arterial compliance (C_T), and thus, its estimation via an accurate and simple method is valuable. Direct noninvasive measurement of C_T is not feasible in the clinical practice. Previous methods exist for indirect estimation of C_T , which, however, require noninvasive, yet complex and expensive, recordings of the central pressure and flow. Here, we introduce a novel, noninvasive method for estimating C_T from a single carotid waveform measurement using regression analysis. Features were extracted from the carotid wave and were combined with demographic data. A prediction pipeline was adopted for estimating C_T using, first, a feature-based regression analysis and, second, the raw carotid pulse wave. The proposed methodology was appraised using the large human cohort ($N = 2,256$) of the Asklepios study. Accurate estimates of C_T were yielded for both prediction schemes, namely, $r = 0.83$ and normalized root mean square error (nRMSE) = 9.58% for the feature-based model, and $r = 0.83$ and nRSME = 9.67% for the model that used the raw signal. The major advantage of this method pertains to the simplification of the technique offering easily applicable and convenient C_T monitoring. Such an approach could offer promising applications, ranging from fast and cost-efficient hemodynamical monitoring by the physician to integration in wearable technologies.

NEW & NOTEWORTHY This article introduces a novel artificial intelligence method to estimate total arterial compliance (C_T) via exploiting the information provided by an uncalibrated carotid blood pressure waveform as well as typical clinical variables. The major finding of this study is that C_T , which is usually acquired using both pressure and flow waveforms, can be accurately derived by the use of the pressure wave alone. This method could potentially facilitate easily applicable and convenient monitoring of C_T .

artificial neural network; machine learning; noninvasive monitoring; pulse wave analysis; vascular aging

INTRODUCTION

In a progressively aging population, it is of utmost importance to develop reliable, noninvasive, and cost-effective tools for estimating relevant biomarkers that can be indicative of cardiovascular risk. Numerous invasive and noninvasive markers have been researched, but there is still the need for additional structural and functional parameters that would be able to assess cardiovascular risk (1). The total arterial compliance (C_T) is a biomechanical property of the arterial tree with great physiological and pathological importance (2–4). C_T and peripheral resistance constitute a major part of the arterial load on the heart (5). Arterial compliance expresses the ability of the arterial system to store blood during systole without excessive pressure rise and influences central blood pressure (6) and stroke volume (7). The C_T is becoming a promising parameter for evaluating assessment

of the relationship between structural and functional changes in the vascular system with respect to its elasticity and capacity (8, 9). Alterations in arterial compliance are associated to various physiological (aging) (10) or pathological (hypertension) conditions (11), which cannot be necessarily assessed by current biomarkers. Importantly, C_T has been found to be superior over traditional evaluation techniques including pulse pressure and echocardiography (9, 11). In addition, other studies have shown that C_T was proven capable of differentiating among diseased, elderly, and healthy individuals (10–12). In view of the emerging evidence on the importance of C_T (8), the development of an accurate and simple method for its estimation may be valuable.

Direct noninvasive measurement of C_T is not feasible in the clinical practice. Several methods have been proposed for indirect estimation of C_T (13–16). Most commonly, these



methods require simultaneous recordings of the proximal aortic pressure and flow waves. Some of the most reliable and accurate techniques include the decay time method (DTM), the area method (AM), and the pulse pressure method (PPM), (15, 17). The principle of the DTM is that during diastole, there is no inflow from the heart, and thus, the decrease of aortic pressure is characterized by the decay time. This decay can be fitted monoexponentially to any portion of the diastole to yield the characteristic time or time constant, which is RC_T , where R is a known value of peripheral resistance (17). The AM was introduced by Randall et al. (18), and it essentially represents an integral variation of the exponential decay method. Compliance is calculated from $RC_T = \int_{t_1}^{t_2} P dx / (P_1 - P_2)$, where P_1 and P_2 are diastolic pressure at time points t_1 and t_2 , respectively. The PPM is based on the fact that the modulus of the input impedance of the arterial system is represented very well by the two-element Windkessel model for the low frequencies (1st to 5th harmonic). Therefore, the pulse pressure will be similar in the true arterial system and the two-element Windkessel model. The PPM uses an iterative process that yields the value of C_T that gives the best fit between the measured pulse pressure and the pulse pressure predicted by the two-element Windkessel model.

Yet, the invasive nature, lack of convenience, and high cost of the required measurements have limited the assessment of C_T , namely, the inverse of arterial stiffness, in everyday clinical practice, whereas surrogates of local or regional arterial stiffness have been applied commonly (16, 19). Measurement of carotid-femoral pulse wave velocity (cfPWV) is considered as the gold standard to evaluate arterial stiffness (20).

Recent advances in machine learning (ML) have expanded the areas and the opportunities in developing novel modeling and predictive methods for clinical use (21). In a previous study, Tavallali et al. (22) proposed and validated a method for estimating cfPWV from the carotid waveform and clinical parameters using neural networks. Their results showed that this approach can provide accurate estimates of cfPWV, offering an advancement in the assessment of arterial stiffness via cfPWV.

In view of these nascent opportunities, the present study introduces a novel, noninvasive, cost-efficient method for estimating C_T from a single carotid waveform measurement using regression analysis. The proposed methodology uses an uncalibrated carotid blood pressure waveform that is subsequently calibrated using the brachial blood pressure values. Features are extracted from the carotid wave and are combined with readily available clinical parameters such as age, sex, height, and weight. A prediction pipeline is adopted for estimating C_T using, first, a feature-based regression analysis and, second, the raw carotid pulse wave. A main advantage of this method pertains to the avoidance of aortic blood flow recording that is commonly required by prior C_T estimators. Given that accurate values of C_T are cumbersome to obtain in the intact organism, in this study, the accuracy of the predictive model was evaluated by comparing the predictions against the C_T values that were derived using the precise and extensively validated PPM (14, 15, 23).

MATERIALS AND METHODS

Asklepios Database

Human data were available from the Asklepios study, a broad prospective longitudinal study with the aim of assessing the development and progression of cardiovascular disease (24). A total of 2,404 subjects were found eligible to be included in the study. The participants underwent a noninvasive evaluation of central hemodynamics, including recordings of carotid blood pressure and aortic blood flow waveforms. The inclusion and exclusion criteria are listed in Table 1. The study protocol was approved by the ethical committee of Ghent University Hospital, and written informed consent of participation was given by all subjects. A comprehensive description of the Asklepios data can be found in the original publication (24).

Measurement of Pressure and Flow Waves

Blood pressure recordings were performed at the left common carotid artery via applanation tonometry using a Millar pen-type tonometer (SPT 301; Millar Instruments, Houston, Texas). The measurement setup, processing, and calibration procedure (based on sphygmomanometer systolic and diastolic blood pressure and applanation tonometry at the brachial artery) were previously described in detail (24, 25).

The carotid pressure was derived as a “mean” waveform of multiple beats from a 20-s recording (6). Pressure data were recorded in continuous sequences of 20 s. The postprocessing included signal filtering (Savitsky–Golay filter, MATLAB, The MathWorks Inc.). Subsequently, identification of individual cycles, detrending (i.e., linearly smoothing out eventual differences in the numerical value of the start and end of the cycle), and averaging were performed. The cycles with a cycle length shorter or longer than 20% of the mean cycle duration were automatically deselected. The same applied for cycles with a shape surpassing the “envelope” curves, which were constructed from the average \pm (two times the standard deviation). The process was repeated iteratively until all cycles were within the “envelope” curves. As an arbitrary quality criterion, data were accepted only if minimally 10 cycles were retained. The average of these cycles was considered as the tonometry recording for the carotid artery. The carotid waveform was calibrated by assuming that diastolic and mean BP values remain fairly constant for the major arteries.

Flow at the aorta was measured using ultrasound (VIVID 7; GE Vingmed Ultrasound, Horten, Norway) from the cross-sectional area and blood velocities in the left ventricular outflow tract (LVOT). The internal diameter of the LVOT was measured in the parasternal long-axis view at the valve annulus, and LVOT area was calculated assuming a circular cross section. Flow velocities were obtained in the LVOT via pulsed-wave Doppler in the apical five-chamber view. Images were exported in raw DICOM format and processed offline within a dedicated software interface in MATLAB (The MathWorks, Natick, MA). For each cardiac cycle, the onset and end of systolic ejection were visually delineated with two cursors, after which the contours in the systolic phase were automatically traced using the transition in pixel intensity above a user-defined threshold value. Two to three

Table 1. *Asklepios inclusion and exclusion criteria*

Inclusion Criteria	
1.	Volunteers, men and women
2.	Aged 35–55 yr at study initiation
3.	Domicile, Erpe-Mere or Nieuwerkerken
Exclusion Criteria	
1.	Clinical presence of atherosclerosis/atherothrombosis
a.	Atherosclerosis: symptomatic or hemodynamically significant (>50% stenosis) presence of atherosclerosis in any major vascular bed
b.	Atherothrombosis: acute coronary syndromes, cerebrovascular thrombosis
c.	Previous or planned revascularization procedure (carotid, coronary, lower limb)
2.	Major concomitant illness
a.	Cardiac: cardiomyopathy/heart failure, significant valvular disease, previous cardiac surgery, (complex) congenital heart disease, heart transplant
b.	Organ failure: end-stage renal disease, hepatic insufficiency, previous organ transplant
c.	Malignant tumors (recently diagnosed or currently treated, with <3 years tumor-free follow-up or tumors that are metastatic or initial treatment was not curative)
d.	Other conditions in which the screening physician expected a life expectancy <5 years
3.	Diabetes mellitus
a.	Diabetes mellitus type 1.
b.	Diabetes mellitus type 2 if confirmed macrovasculopathy (see exclusion criterion 1) or significant renal impairment (see exclusion criterion 2 b)
4.	Specific conditions precluding accurate hemodynamic assessment
a.	Continually irregular cardiac cycle: atrial fibrillation
b.	State of hyperdynamic activity: pregnancy (in the preceding 6 mo)
5.	Inability to provide informed consent.

cycles were averaged, and the average cycle subsampled to 500 sample points and smoothed using a Savitsky–Golay filter (order 3, frame width 31). The maximal velocities were multiplied with the LVOT cross-sectional area to obtain the aorta flow waveform (assuming a flat velocity profile in the LVOT). This approach yielded physiologically relevant values of stroke volume and cardiac output (2).

The heart rate (HR) was calculated from the average duration of pressure and flow signals. The time vectors of the two signals were normalized, synchronized, and then denormalized, rendering the heart cycle length equal to the average length of the pressure and flow waveform.

Derivation of the Reference Compliance

Measurement of the real C_T values in a human cohort is not feasible. In the present study, the pulse pressure method (PPM) was used as the ground truth value for compliance (23). The PPM is based on the fact that the modulus of the input impedance of the arterial system is represented very well by the two-element Windkessel model for the low frequencies (1st to 5th harmonic). Therefore, the pulse pressure will be similar in the true arterial system and the two-element Windkessel model. From the ratio of mean pressure over mean flow, we derive peripheral resistance. Then, using measured flow as input to the two-element Windkessel, the predicted pulse pressure is fit to the actual pulse pressure by adjusting compliance. Compliance adjustment is done by a simple “trial and error” type of approach knowing that lower compliance yields larger pulse pressures. Following an iterative process, the value of the compliance (C_T) that gives the best fit of the measured pulse pressure provides the estimate of the compliance. The method has been thoroughly validated both in silico under various hemodynamical states (17, 23) and against in vivo data (14) and it has been proven to be capable of accurately estimating arterial compliance.

Features Extraction from the Carotid Pressure Wave

Features were extracted from the carotid pressure signal and its time derivative (Fig. 1). Concretely, the features included the systolic blood pressure (SBP), the diastolic blood pressure (DBP), the dicrotic notch pressure point (P_{DN}), the dicrotic notch time point (t_{DN}), the upstroke systolic area ($A_{upstroke}$), the total systolic area ($A_{systolic}$), the diastolic area ($A_{diastolic}$), the peak of time derivative (dp/dt_{max}), the time point that peak derivative occurs ($t_{dp/dt_{max}}$), and the heart rate (HR).

Regression Analysis

The extracted features, i.e., SBP, DBP, MAP, PP, P_{DN} , t_{DN} , $A_{upstroke}$, $A_{systolic}$, $A_{diastolic}$, dp/dt_{max} , $t_{dp/dt_{max}}$, HR, as well as demographic data including age, sex, height, and weight were used as the input features to the ML model. The C_T (as derived from PPM) was set to be the target output variable. The data were organized in pairs (inputs-outputs) and were kept for the training/testing process. For the regression process, we used an artificial neural network (ANN) and a linear regressor (LR) to estimate the target variable of interest. Furthermore, the performance of a predictive model including cardiac output (CO) as an additional input feature was assessed. It should be noted that the models including the CO feature are not considered as the main focus of the present study. We, however, decided to include them in the analysis for investigating the importance of CO in the estimations. For the ANN, a fixed one-hidden layer structure was selected and the “Adam” optimizer was used (26). In addition, the ANN was trained/tested using as input the entire raw carotid waveform, as well as demographic data. The carotid BP waveforms were sampled at 100 data points per cycle. The predictive models are summarized in Table 2.

Of the 2,404 participants, 148 were excluded due to missing or erroneously measured data. Their exclusion led to a final size population equal to 2,256 participants. The data

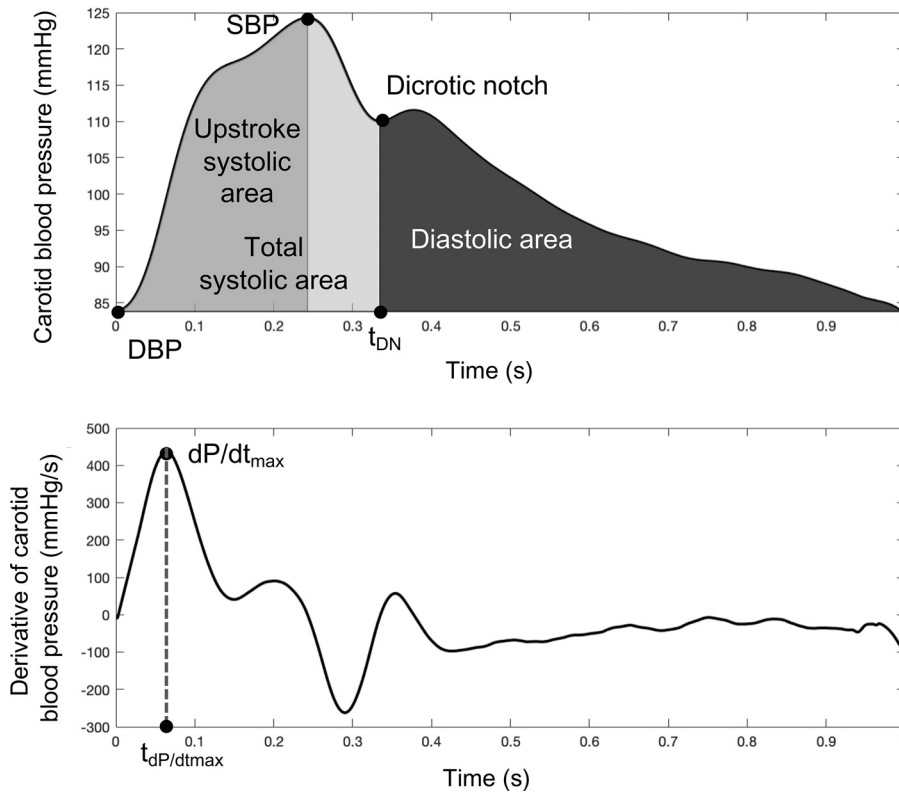


Figure 1. Indication of features on the carotid pressure waveform and the time derivative.

were randomly split into three sets: a training set (80% of the total data set), a validation set (10%), and a test set (10%). Therefore, out of the entire cohort, 1,796 subjects were used for the training, 223 data instances were used as validation for the hyperparameter selection, and 237 subjects were kept for the testing. To mitigate overfitting and to increase the generalization capacity, the model should be trained for optimal hyperparameter values. For the ANN, the batch size (defines the number of samples that will be propagated through the network) was set to be equal to 200, whereas the number of epochs was optimized. The number of epochs defines the number of times that the learning algorithm works through the entire training data set. For selecting the optimal value for epochs, we computed the training loss and the validation loss for various values of epochs. Here, the loss corresponds to the mean square error (MSE). Loss values were monitored by early stopping call back function. When an increment is observed in the loss values, training

comes to halt and the respective value of epoch indicates the optimal selection. All the yielded optimized hyperparameters are aggregated in Table 3. Subsequently, the test set was fed into the trained models to predict C_T and the precision was evaluated.

The current study aimed to evaluate the importance of each input feature for the C_T prediction. The importance was quantified by the use of the permutation feature importances (27). The concept of permutation feature importances relies on measuring the importance of a feature by calculating the increase in the prediction error after permuting the feature. The permutation importances were computed by shuffling the values of each feature on the test set and by estimating the RMSE after the permutation. This process was repeated 20 times, and the mean and standard deviation of the increase in RMSE were reported. Subsequently, an additional ANN was trained/tested using the five most important features yielded by the aforementioned analysis.

Table 2. Summary of all the ML models trained/tested based on their inputs

Model	Inputs	Input Vector Size
LR1	SBP, DBP, MAP, PP, P_{DN} , t_{DN} , $A_{upstroke}$, $A_{systolic}$, $A_{diastolic}$, dP/dt_{max} , $t_{dP/dt_{max}}$	16
LR2	SBP, DBP, MAP, PP, P_{DN} , t_{DN} , $A_{upstroke}$, $A_{systolic}$, $A_{diastolic}$, dP/dt_{max} , $t_{dP/dt_{max}}$, HR, age, sex, height, weight, CO	17
ANN1	SBP, DBP, MAP, PP, P_{DN} , t_{DN} , $A_{upstroke}$, $A_{systolic}$, $A_{diastolic}$, dP/dt_{max} , $t_{dP/dt_{max}}$	16
ANN2	SBP, DBP, MAP, PP, P_{DN} , t_{DN} , $A_{upstroke}$, $A_{systolic}$, $A_{diastolic}$, dP/dt_{max} , $t_{dP/dt_{max}}$, HR, age, sex, height, weight, CO	17
ANN3	Entire raw carotid pressure waveform, HR, age, sex, height, weight	105
ANN4	Entire raw carotid pressure waveform, HR	101
ANN5	PP, SBP, $A_{diastolic}$, $A_{systolic}$, weight (most important features)	5

$A_{diastolic}$, diastolic area; ANN, artificial neural network; CO, cardiac output; DBP, diastolic blood pressure; t_{DN} , dicotic notch time point; HR, heart rate; LR, linear regression; MAP, mean arterial pressure; ML, machine learning; P_{DN} , dicotic notch pressure point; dP/dt_{max} , peak of time derivative; PP, pulse pressure; SBP, systolic blood pressure; $A_{systolic}$, $t_{dP/dt_{max}}$, time point of peak derivative; total systolic area; $A_{upstroke}$, upstroke systolic area.

Table 3. Optimal number of epochs for each ANN

C _T Models	Epochs
ANN1	118
ANN2	380
ANN3	187
ANN4	212
ANN5	101

ANN, artificial neural network; C_T, total arterial compliance.

The training/testing pipeline as well as the preanalyses and postanalyses were implemented using the Scikit-learn library (28) in a Python programming environment. The Pandas and Numpy packages were also used (29, 30).

Sensitivity to Noise and Variations in the Wave Morphology

We further evaluated the robustness of the method in the case of measurement noise or variations in the morphology of the wave. The evaluation was done following two controlled experiments. First, errors were considered for the extraction of the wave-based features for the ANN1 model. Concretely, errors in features were simulated with a random distribution. The error for each variable was randomly drawn from the range of (−5, +5)%. Subsequently, each variable value was multiplied with a noise factor; for instance, for a randomly selected error of −4%, the respective variable value was multiplied with a noise factor equal to 0.96. The process was repeated for the noise ranges of ±7% and ±10%. Second, we wished to simulate adverse effects for the ANN3 by distorting the shape of the input pressure wave. This was achieved by adding white Gaussian noise assuming three signal-to-noise ratio (SNR) values, i.e., 40, 35, and 30 dB. Selection of the SNR values was done experimentally so that an obvious distortion in the wave morphology is achieved that could render the model incapable of making a correct prediction. A lower SNR value would lead to an unrealistically signal variation that would be inappropriate to use and thus would be discarded. A higher SNR value would make it easy for the model to yield a precise estimation.

Statistical Analysis

All data are presented as means ± SD. The statistical analysis was performed in Python (Python Software Foundation, Python Language Reference, v. 3.6.8, available at <http://www.python.org>). The accuracy between the estimates and the reference values was evaluated with the Pearson's correlation coefficient (*r*) and the normalized root mean square error (nRMSE). Bias and limits of agreement (LoA) (where 95% of errors are expected to lie) were calculated using the Bland–Altman analysis (31). The computed nRMSE was based on the difference between the minimum and maximum values of the dependent variable *y* and was computed as RMSE/(*y*_{max} − *y*_{min}). Level of statistical significance was set equal to 0.05.

RESULTS

The population consisted of 1,087 (48%) male participants and 1,169 (52%) female participants. The distributions of the

cardiovascular parameters of the study cohort (*N* = 2,256) are presented in Table 4.

Comparison between the Model-Predicted and Reference Data

The scatterplots and the Bland–Altman plots of the estimated C_T for each of the models against the ground truth are shown in Figs. 2 and 3. Regression metrics for the agreement, precision, and bias are aggregated in Table 5. The regression slopes were similar for the LRI, ANN1, and ANN3 in which the demographic data were considered as inputs. Accuracy was significantly increased for the models that used CO as an input feature (*r* ≥ 0.94). Variability of the absolute errors between predicted and actual compliance values was low for the LRI, ANN1, and ANN3. In all models, LoA were narrow and biases were reported to be close to zero. Table 6 presents the feature importances of the input regressors for C_T, respectively. Among the inputs, PP, SBP, and A_{diastolic} appeared to have the highest importance levels (error increase was more than 0.20 mL/mmHg). On the other hand, P_{DN} and A_{upstroke} had the lowest importance levels (error increased by 0.01 mL/mmHg). The ANN5 using only the five top-contributing features had a satisfactory performance similar to the one of ANN1 that used all the extracted wave-based features and the performance of ANN3 that was fed with the entire waveform and the demographical data (nRMSE was found to be close to 10% and correlation equal to 0.82).

Sensitivity to Noise and Variations in the Wave Morphology

An input carotid pressure wave with the simulated artificial noise is illustrated in Fig. 4. The addition of artificial noise affected the wave's shape, harming the smoothness of

Table 4. Description of the cardiovascular characteristics and parameters of the study cohort

Variable	Value
<i>N</i>	2,256
Age, yr	45.91 ± 5.98
Height, cm	169.18 ± 8.82
Weight, kg	73.65 ± 14.45
Carotid SBP, mmHg	130.96 ± 10.90
Carotid DBP, mmHg	77.36 ± 16.83
Carotid PP, mmHg	53.59 ± 11.82
Mean arterial pressure, mmHg	99.60 ± 12.04
Cardiac output, L/min	4.95 ± 1.16
Heart rate, beats/min	60.35 ± 8.94
Total arterial compliance, mL/mmHg	1.00 ± 0.32
Total peripheral resistance, mmHg·s/mL	1.27 ± 0.34
P _{DN} , mmHg	110.38 ± 13.50
<i>t</i> _{DN} , s	0.38 ± 0.05
A _{upstroke} , mmHg·s	26.21 ± 7.00
A _{systolic} , mmHg·s	43.38 ± 8.03
A _{diastolic} , mmHg·s	58.58 ± 13.00
dP/d <i>t</i> _{max} , mmHg/s	657.07 ± 160.08
<i>t</i> _{dP/d<i>t</i>max} , s	0.068 ± 0.014

Values are means ± SD; *N*, number of participants. A_{diastolic}, diastolic area; DBP, diastolic blood pressure; P_{DN}, dicrotic notch pressure point; *t*_{DN}, dicrotic notch time point; dP/d*t*_{max}, peak of time derivative; PP, pulse pressure; SBP, systolic blood pressure; *t*_{dP/d*t*max}, time point of peak derivative; A_{systolic}, total systolic area; A_{upstroke}, upstroke systolic area.

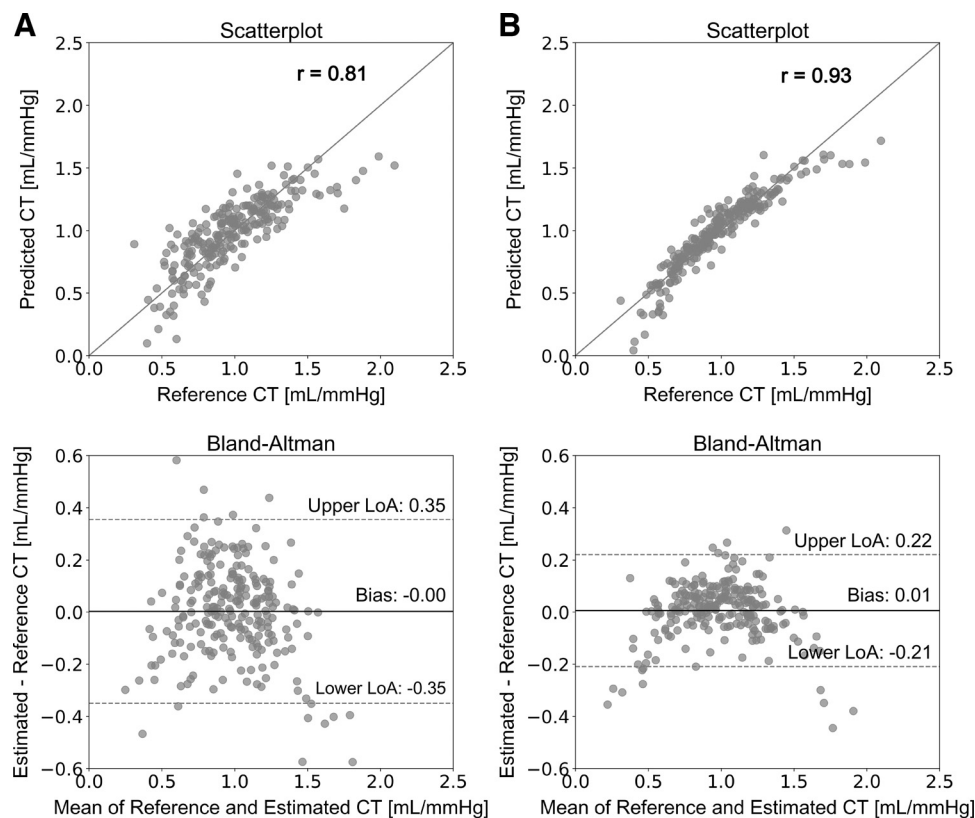


Figure 2. Comparison between predicted and reference data. Scatterplot and Bland–Altman plot between the predicted C_T and the reference C_T for LR1 (A) and LR2 (B). The solid line of the scatterplots represents equality. In Bland–Altman plots, limits of agreement (LoA) are defined by the two horizontal dashed lines. C_T , total arterial compliance; LR, linear regression.

the curve and leading to variations in the peaks. We can observe that for an SNR = 20 dB (Fig. 4C), it begins to become difficult to clearly distinguish the shape. As anticipated, the agreement and correlation between the estimated C_T and the reference C_T decreased with the increase in the noise level. Table 7 reports the correlation coefficients and normalized RMSE values as a function of the noise levels for the two simulated experimental settings.

DISCUSSION

This article introduces a novel ML method for estimating C_T . The findings indicated that arterial compliance can be accurately predicted by exploiting the carotid blood pressure waveform. This method relies on the raw information hidden in the carotid pulse wave that can be unveiled via the sophisticated ML capacity. In addition, the present study introduces an ANN estimator that is based on features extracted from the carotid wave. These features appeared to be powerful predictors of C_T . The major advantage of a method for estimating C_T from a single carotid pressure waveform is that it eliminates the need for a flow or velocity recording that requires complex and expensive echocardiographic or magnetic resonance imaging procedures. Consequently, it provides a faster and more convenient way for monitoring arterial compliance.

The C_T together with the total vascular resistance are the two major parameters that describe the global biomechanical properties of the arterial system. Modeling vasculature and hemodynamical responses often require the estimation of C_T , whereas other methods for minimally invasive cardiac

output monitoring (namely, pulse contour analysis) are also dependent on C_T values (32). Yet, despite the additional clinical utility of C_T , current techniques for C_T have not entered the everyday clinical practice. This is mainly attributed to inherent limitations, including methodological complexity and expensiveness.

Moreover, the lack of a common basis and guidelines has hampered the establishment of C_T as an outcome predictor. However, several studies have demonstrated that assessment of C_T is valuable for not only cardiovascular risk evaluation but also assessment of the relationship between structural and functional changes in the vascular system with respect to its elasticity [14, 33]. Moreover, Haluska et al. (9) stressed that derivation of C_T adds incremental benefit to Framingham risk scores in patients with intermediate cardiovascular risk. Hence, C_T is becoming a valuable parameter in the clinical setting by providing additive value in conjunction with other vascular characteristics (12) or by acting as a superior predictor over current traditional techniques (9). The suggested method could potentially facilitate the further elucidation of the clinical utility of C_T as a risk predictor.

The current study trained and tested two ML models of different nature, namely, a typical linear regressor and an artificial neural network. There was no significant variability in the errors among the two models for the feature-based configurations, i.e., LR1 and ANN1 [LoA were (−0.35, 0.35) and (−0.33, 0.34) mL/mmHg]. However, the LR1 could not account for the nonlinear relationships between the inputs and the compliance, and this led to curvilinearity in the results' plots. Importantly, there is much additive value offered by the ANN estimator that has been proven capable

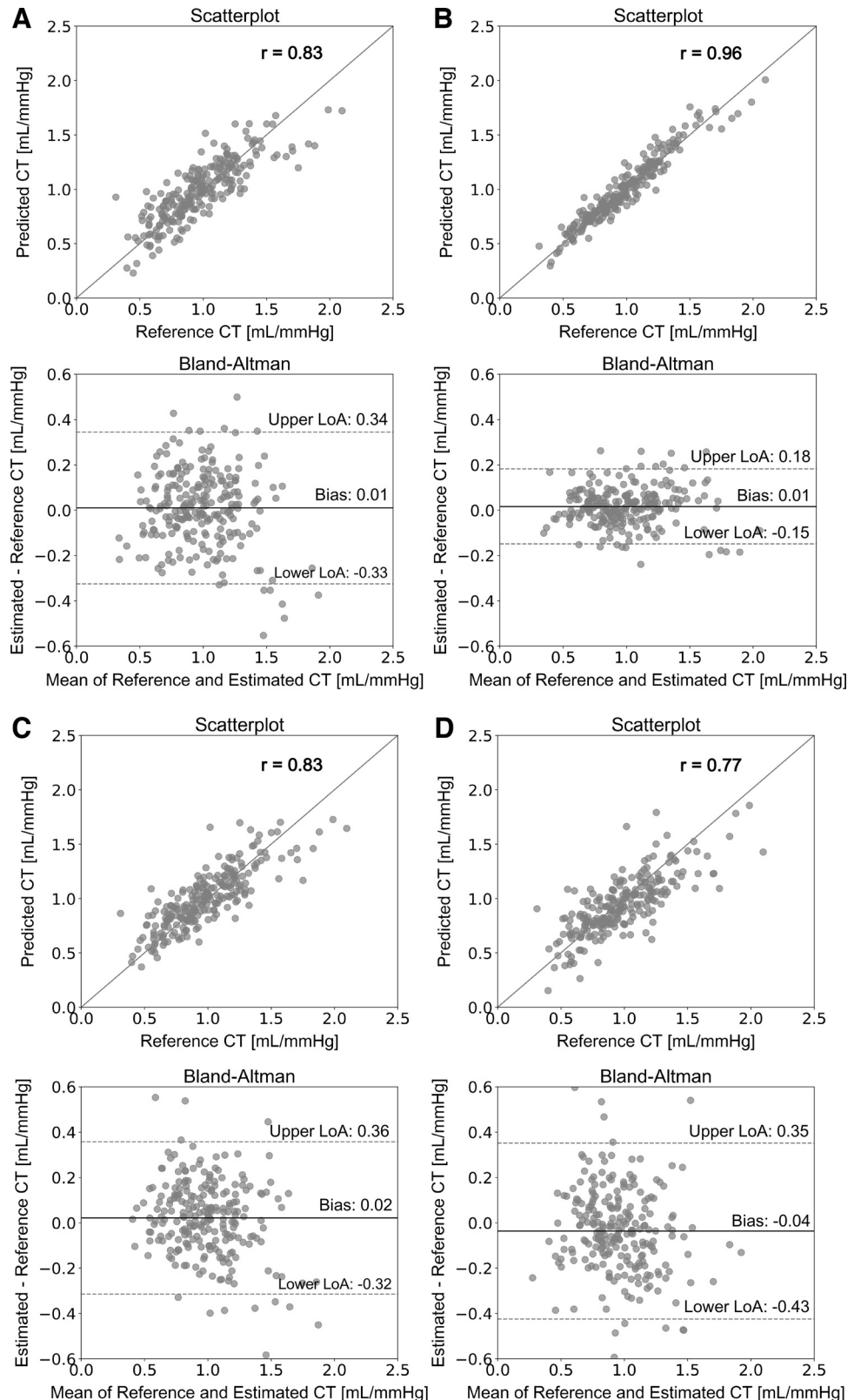


Figure 3. Comparison between predicted and reference data. Scatterplot and Bland–Altman plot between the predicted C_T and the reference C_T for ANN1 (A), ANN2 (B), ANN3 (C), and ANN4 (D). The solid line of the scatterplots represents equality. In Bland–Altman plots, limits of agreement (LoA) are defined by the two horizontal dashed lines. ANN, artificial neural network; C_T , total arterial compliance.

of accurately predicting C_T from the raw blood pressure waveform. This approach could introduce a greatly promising method for the medical community by reducing the cost and the complexity in assessing C_T . Moreover, as

anticipated, the inclusion of CO in the input vector essentially increased the precision of the results. Compliance is a measure of volume change against unit pressure change. Hence, the two parameters are highly interdependent. The

Table 5. Regression statistics between model-predicted and reference C_T data

Model	Slope	Intercept, mL/mmHg	r	P Value	nRMSE, %	Bias (LoA), mL/mmHg	Predicted C_T , mL/mmHg
LR1	0.71	0.29	0.81	<0.0001	10.63	-0.00 (-0.35, 0.35)	0.98 ± 0.28
LR2	0.93	0.07	0.93	<0.0001	6.13	0.01 (-0.21, 0.22)	0.99 ± 0.3
ANN1	0.77	0.24	0.83	<0.0001	9.58	0.01 (-0.33, 0.34)	0.99 ± 0.28
ANN2	0.97	0.05	0.96	<0.0001	4.8	0.01 (-0.15, 0.18)	1 ± 0.3
ANN3	0.73	0.28	0.83	<0.0001	9.67	0.02 (-0.32, 0.36)	1 ± 0.27
ANN4	0.68	0.28	0.77	<0.0001	11.26	-0.04 (-0.43, 0.35)	0.94 ± 0.27
ANN5	0.74	0.26	0.82	<0.0001	9.9	0.01 (-0.34, 0.36)	0.99 ± 0.27

ANN, artificial neural network; C_T , total arterial compliance; LoA, limits of agreement; LR, linear regression; nRMSE, normalized root mean square error; r , Pearson's correlation coefficient. Two-sided P value for a hypothesis test whose null hypothesis is that the slope is zero, using Wald test with t distribution of the test statistic.

dependency in conjunction to the blood pressure information allows for computing one from the other. This is a principle applied by several existing methods. In addition, providing that the PPM (used to derive the reference C_T) uses the aortic flow for the C_T calculation, introducing the aortic flow information to the ML model would inarguably reduce the error. Nevertheless, our study's objective is to provide estimates of C_T without the need for the aortic flow or velocity recording (and thus CO).

It is of importance to recognize the contribution of each input to the prediction of C_T . The PP was found to have the highest influence on the prediction error, namely, 0.31 ± 0.04 mL/mmHg for C_T values within a range of 0.3–2.1 mL/mmHg. This is highly anticipated given that PP is essentially determined by the elastic properties of the aorta (34). Due to the topological proximity of the carotid artery to the aorta, the carotid PP constitutes a fair surrogate of the aortic PP. Hence, the strong interdependence between the PP and C_T is also in effect for the carotid pressure. Moreover, one should not ignore the fact that the PPM, which was applied for acquiring the compliance values, relies on an iterative process that yields the C_T with the best fit in terms of PP. The SBP also appeared to impact the accuracy of the estimation by an error increase of 0.28 ± 0.02 mL/mmHg. The PP and SBP were followed by $A_{\text{diastolic}}$ and A_{systolic} . The combination of the latter yields the entire area under the curve whose measurement is involved in the arterial pulse contour analysis for CO estimation (32); knowledge of MAP and a notion of CO allows for approximating arterial compliance. Moreover, the substantial contribution of the $A_{\text{diastolic}}$

may be attributed to its association to the decay time constant ($\tau = RC_T$) whose concept is used by the AM for estimating compliance. The demographic information, and in particular weight, had a high importance level for the C_T estimator. This was also observed from the reduced precision of the predictive model that excluded the individual's demographic data from the input vector (ANN4) where the correlation was decreased to 0.77. Arterial compliance has been shown to be highly dependent on arterial geometry that is determined by the body size, and thus weight and height. When only the most important features were used in ANN5 (permutation importance higher than 0.1 mL/mmHg), the accuracy remained similarly high as one of the ANNs that used either all the extracted features (ANN1) or all the wave points (ANN3). Therefore, it should not be necessary to use a higher number of input features for the C_T predictive models. Finally, the lower importance levels of some inputs might be explained by the fact that the information embedded in their values may be contained already in other inputs with higher importance levels.

Estimation of cfPWV using the proposed methodology would yield a correlation equal to 0.6 between the estimated and the reference values (data not shown). It is likely that the lower correlation is attributed to the fact that the method uses as input a waveform from a single arterial site, whereas measurement of the foot-to-foot cfPWV requires waves from two arterial locations. Nevertheless, cfPWV can be measured in an easy and noninvasive way with satisfactory reproducibility, and hence, further simplification of its acquisition would not add tremendously to the current state of the art. In contrast, fast, convenient, and cost-efficient determination of C_T is still missing.

In this study, we chose to use a single carotid pressure waveform for estimating arterial compliance. The rationale behind the use of a single wave relies on the current function of the existing devices. The current commercial devices (e.g., SphygmoCor) collect multiple recordings of the pressure wave for a specific time window and then yield an average blood pressure wave for the subject under consideration. Ideally, our algorithm could be embedded into such a device and provide the additional approximation of arterial compliance. In such a setting, a single carotid waveform would be sufficient. However, as variations may occur across several beats of measurement, it is possible that the C_T prediction is influenced. Yet, the sensitivity analysis demonstrated that small alterations in the wave's morphology due to noise do not affect significantly the predictions for an SNR equal to

Table 6. Permutation feature importances for the ANN1

Feature	+ δ RMSE, mL/mmHg	Feature	+ δ RMSE, mL/mmHg
PP	0.31 ± 0.04	P_{DN}	0.04 ± 0.01
SBP	0.28 ± 0.02	MAP	0.03 ± 0.01
$A_{\text{diastolic}}$	0.24 ± 0.02	dP/dt_{max}	0.02 ± 0.00
A_{systolic}	0.14 ± 0.02	HR	0.02 ± 0.01
Weight	0.11 ± 0.01	$t_{dP/dt_{\text{max}}}$	0.02 ± 0.01
DBP	0.07 ± 0.01	Age	0.02 ± 0.00
Height	0.05 ± 0.01	t_{DN}	0.01 ± 0.00
Sex	0.04 ± 0.01	A_{upstroke}	0.01 ± 0.01

ANN, artificial neural network; $A_{\text{diastolic}}$, diastolic area; DBP, diastolic blood pressure; P_{DN} , diastolic notch pressure point; t_{DN} , diastolic notch time point; HR, heart rate; MAP, mean arterial pressure; dP/dt_{max} , peak of time derivative; PP, pulse pressure; RMSE, root mean square error; SBP, systolic blood pressure; $t_{dP/dt_{\text{max}}}$, time point of peak derivative; A_{systolic} , total systolic area; A_{upstroke} , upstroke systolic area.

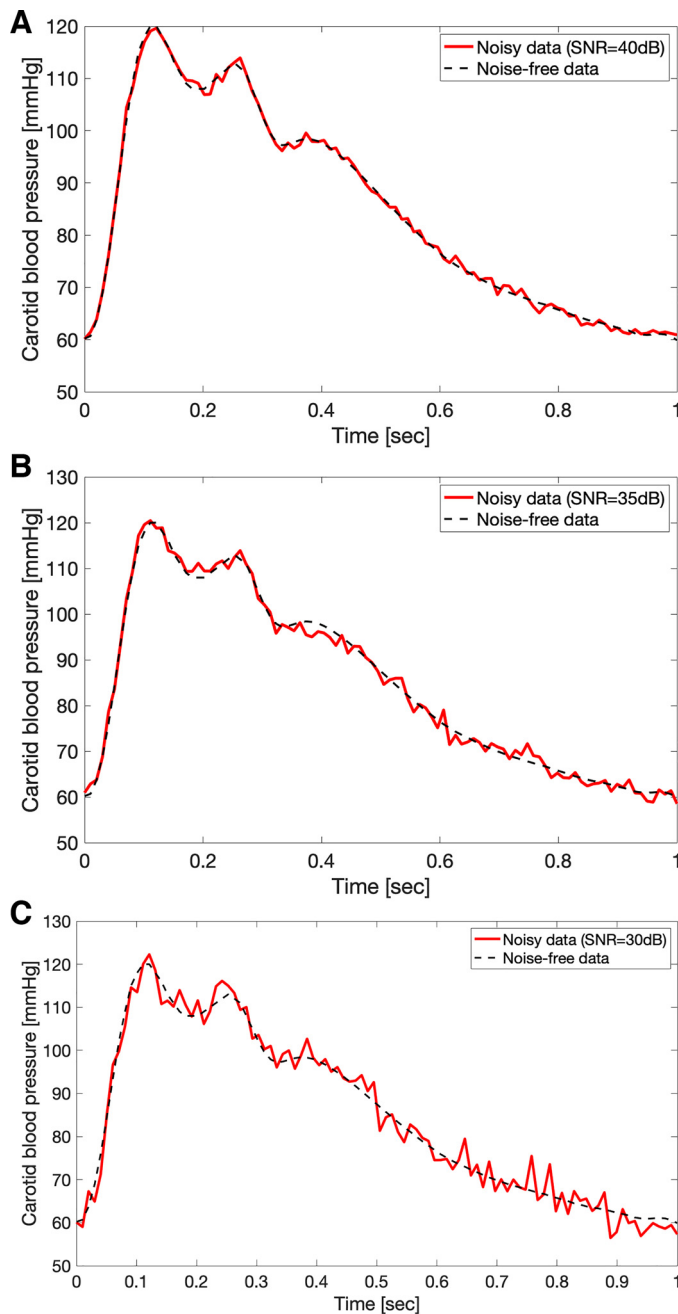


Figure 4. Carotid blood pressure waves after adding artificial noise, assuming SNR = 40 dB (A), SNR = 35 dB (B), and SNR = 30 dB (C). The noisy data are presented in red solid lines and the original noise-free data in black dashed lines.

40 dB. Validation of the methodology using multiple beats of carotid pressure remains to be conducted to quantify the effect of such variations in vivo.

The BP waveform has been shown to be crucial for assessing the vascular state in the human. It provides outstanding information on central hemodynamics, microcirculation and macrocirculation cross talk, and arterial stiffness (2–4, 35, 36). Moreover, signal processing techniques are rapidly advancing allowing for creating a gold mine of physiological information hidden in pressure blood waveform. In this study, we evaluated the performance of ML models on

revealing the hidden information related to arterial compliance in commonly used pressure wave features. Furthermore, we tested the unveiling capacity of an ANN that was fed with the raw pressure signal and received no guidance regarding the input features to use for the training/testing process. Interestingly, the algorithm performed very satisfactorily when the raw carotid waveform was prescribed to the ANN input layer. These findings indicate the beginning of a new era where the ML algorithms are capable of revealing more sophisticated pieces of vascular information through learning by itself from the available clinical data.

Undoubtedly, noninvasive health monitoring technology is on the frontiers of modern healthcare, and it is bound to expand inside and beyond the clinical environment. Concurrently, the rapid advance of wearable technologies is transforming the healthcare system on a global scale. Blood pressure sensing devices aim to be essentially miniaturized, whereas their function will be highly assisted by pressure wave analysis techniques. In this context, reducing the required measurements to only a single waveform in conjunction with the greatly promising potential of signal processing techniques creates a unique opportunity for future use in the market. In addition, medical consultation is expected to become available remotely at all times by connecting to the data cloud where specialized clinicians will be interpreting the available parameters.

Limitations

A main limitation of this study is that the values for C_T , which were used as the ground truth, were derived using the PPM. Unarguably, this value does not correspond to the actual arterial compliance. Nonetheless, acquisition of the real arterial compliance would not be feasible in an intact organism. In addition, the PPM has been shown to provide reliable compliance estimations and, therefore, it constitutes a trustworthy alternative for validating our method (14, 15, 23). Another limitation is that the study population included individuals free of cardiovascular disease or pathology. It is not guaranteed that the developed models will be capable of making predictions for patients with, for instance, aortic valve stenosis, arrhythmias, or other pathologies. Future work is needed to validate the proposed methodological framework using such populations. Finally, it is well established that healthy aging and cardiovascular diseases, such

Table 7. Correlation coefficients and nRMSE values as a function of the artificial noise level in the distorted carotid pressure waves for the ANN1 and ANN3 models

Model	r	nRMSE, %
ANN1		
Noise level, %		
±5	0.79	10.73
±7	0.78	11.11
±10	0.71	13.51
ANN3		
SNR, dB		
40	0.8	10.34
35	0.79	10.76
30	0.75	12.36

ANN, artificial neural network; nRMSE, normalized root mean square error; SNR, signal-to-noise ratio.

as hypertension and heart failure, are associated with increased arterial stiffness (37, 38). Therefore, a method that is capable of differentiating between healthy and disease is highly desirable. At this initial stage, we demonstrated that accurate estimations of C_T can be yielded using our ML-based approach. Given that C_T has been found to be capable of differentiating between hypertensive, elderly and healthy individuals (10–12), as a next step, we envision to evaluate the robustness of the proposed method for classifying high-risk populations and finally verify its clinical significance in terms of risk stratification.

Conclusions

This article introduces a novel artificial intelligence method to estimate C_T . The method relies on exploiting the information provided by the carotid blood pressure waveform as well as typical clinical variables (such as demographical data). Our results demonstrated that accurate estimates of C_T can be obtained following our methodology. The importance of the method is based on the simplification of the technique offering easily applicable and convenient monitoring of C_T . Such an approach could provide promising applications that may be integrated in wearable technologies and smartphones. Finally, the study further supports the importance of arterial pulse waves in the assessment of cardiovascular health and suggests the potentiality of ML in advancing the detection of clinical biomarkers in medicine.

DISCLOSURES

No conflicts of interest, financial or otherwise, are declared by the authors.

AUTHOR CONTRIBUTIONS

V.B. conceived and designed research; V.B. performed experiments; V.B. analyzed data; V.B., P.S., and N.S. interpreted results of experiments; V.B. prepared figures; V.B. drafted manuscript; V.B., P.S., G.R., S.P., and N.S. edited and revised manuscript; V.B., P.S., G.R., S.P., and N.S. approved final version of manuscript.

REFERENCES

- Koenig W. Update on integrated biomarkers for assessment of long-term risk of cardiovascular complications in initially healthy subjects and patients with manifest atherosclerosis. *Ann Med* 41: 332–343, 2009. doi:10.1080/07853890902769675.
- Safar ME, London GM. Arterial and venous compliance in sustained essential hypertension. *Hypertension* 10: 133–139, 1987. doi:10.1161/01.hyp.10.2.133.
- Chemla D, Antony I, Lecarpentier Y, Nitenberg A. Contribution of systemic vascular resistance and total arterial compliance to effective arterial elastance in humans. *Am J Physiol Heart Circ Physiol* 285: H614–H620, 2003. doi:10.1152/ajpheart.00823.2002.
- Haluska BA, Jeffriess L, Downey M, Carlier SG, Marwick TH. Influence of cardiovascular risk factors on total arterial compliance. *J Am Soc Echocardiogr* 21: 123–128, 2008. doi:10.1016/j.echo.2007.05.043.
- Elzinga G, Westerhof N. Pressure and flow generated by the left ventricle against different impedances. *Circ Res* 32: 178–186, 1973. doi:10.1161/01.res.32.2.178.
- Segers P, Rietzschel ER, De Buyzere ML, Vermeersch SJ, De Bacquer D, Van Bortel LM, De Backer G, Gillebert TC, Verdonck PR; Asklepios Investigators. Noninvasive (input) impedance, pulse wave velocity, and wave reflection in healthy middle-aged men and women. *Hypertension* 49: 1248–1255, 2007. doi:10.1161/HYPERTENSIONAHA.106.085480.
- Stergiopoulos N, Meister JJ, Westerhof N. Determinants of stroke volume and systolic and diastolic aortic pressure. *Am J Physiol Heart Circ Physiol* 270: H2050–H2059, 1996. doi:10.1152/ajpheart.1996.270.6.H2050.
- Heitmar R. Total arterial compliance: the future of cardiovascular risk assessment? *J Hum Hypertens* 24: 227–229, 2010. doi:10.1038/jhh.2009.106.
- Haluska BA, Jeffries L, Carlier S, Marwick TH. Measurement of arterial distensibility and compliance to assess prognosis. *Atherosclerosis* 209: 474–480, 2010. doi:10.1016/j.atherosclerosis.2009.10.018.
- Van Bortel L, Spek J. Influence of aging on arterial compliance. *J Hum Hypertens* 12: 583–586, 1998. doi:10.1038/sj.jhh.1000669.
- Beltran A. Arterial compliance abnormalities in isolated systolic hypertension. *Am J Hypertens* 14: 1007–1011, 2001. doi:10.1016/S0895-7061(01)02160-4.
- Lind L. Arterial compliance and endothelium-dependent vasodilation are independently related to coronary risk in the elderly: the Prospective Investigation of the Vasculature in Uppsala Seniors (PIVUS) study. *Clin Physiol Funct Imaging* 28: 373–377, 2008. doi:10.1111/j.1475-097X.2008.00816.x.
- Liu Z, Brin KP, Yin FC. Estimation of total arterial compliance: an improved method and evaluation of current methods. *Am J Physiol Heart Circ Physiol* 251: H588–H600, 1986. doi:10.1152/ajpheart.1986.251.3.H588.
- Stergiopoulos N, Segers P, Westerhof N. Use of pulse pressure method for estimating total arterial compliance in vivo. *Am J Physiol Heart Circ Physiol* 276: H424–H428, 1999. doi:10.1152/ajpheart.1999.276.2.H424.
- Segers P, Verdonck P, Deryck Y, Brimiouille S, Naeije R, Carlier S, Stergiopoulos N. Pulse pressure method and the area method for the estimation of total arterial compliance in dogs: sensitivity to wave reflection intensity. *Ann Biomed Eng* 27: 480–485, 1999. doi:10.1114/1.192.
- Mackenzie IS, Wilkinson IB, Cockcroft JR. Assessment of arterial stiffness in clinical practice. *QJM* 95: 67–74, 2002. doi:10.1093/qjmed/95.2.67.
- Stergiopoulos N, Meister JJ, Westerhof N. Evaluation of methods for estimation of total arterial compliance. *Am J Physiol Heart Circ Physiol* 268: H1540–H1548, 1995. doi:10.1152/ajpheart.1995.268.4.H1540.
- Randall OS, Esler MD, Calfee RV, Bulloch GF, Maisel AS, Culp B. Arterial compliance in hypertension. *Aust N Z J Med* 6: 49–59, 1976. doi:10.1111/j.1445-5994.1976.tb03323.x.
- Sakuragi S, Abhayaratna WP. Arterial stiffness: methods of measurement, physiologic determinants and prediction of cardiovascular outcomes. *Int J Cardiol* 138: 112–118, 2010. doi:10.1016/j.ijcard.2009.04.027.
- Laurent S, Cockcroft J, Van Bortel L, Boutouyrie P, Giannattasio C, Hayoz D, Pannier B, Vlachopoulos C, Wilkinson I, Struijker-Boudier H; European Network for Non-invasive Investigation of Large Arteries. Expert consensus document on arterial stiffness: methodological issues and clinical applications. *Eur Heart J* 27: 2588–2605, 2006. doi:10.1093/eurheartj/ehl254.
- Shameer K, Johnson KW, Glicksberg BS, Dudley JT, Sengupta PP. Machine learning in cardiovascular medicine: are we there yet? *Heart* 104: 1156–1164, 2018. doi:10.1136/heartjnl-2017-311198.
- Tavallali P, Razavi M, Pahlevan NM. Artificial intelligence estimation of carotid-femoral pulse wave velocity using carotid waveform. *Sci Rep* 8: 1014, 2018. doi:10.1038/s41598-018-19457-0.
- Stergiopoulos N, Meister JJ, Westerhof N. Simple and accurate way for estimating total and segmental arterial compliance: the pulse pressure method. *Ann Biomed Eng* 22: 392–397, 1994. doi:10.1007/BF02368245.
- Rietzschel ER, De Buyzere ML, Bekaert S, Segers P, De Bacquer D, Cooman L, Van Damme P, Cassiman P, Langlois M, van Oostveldt P, Verdonck P, Backer GD, Gillebert TC; Asklepios Investigators. Rationale, design, methods and baseline characteristics of the Asklepios study. *Eur J Cardiovasc Prev Rehabil* 14: 179–191, 2007. doi:10.1097/HJR.0b013e328012c380.
- Segers P, Rietzschel E, Heireman S, Debuyzere M, Gillebert T, Verdonck P, Bortel LV. Carotid tonometry versus synthesized aorta pressure waves for the estimation of central systolic blood pressure and augmentation index. *Am J Hypertens* 18: 1168–1173, 2005. doi:10.1016/j.amjhyper.2005.04.005.

26. **Kingma DP, Ba J.** Adam: a method for stochastic optimization. In: *The 3rd International Conference for Learning Representations*, San Diego, US, 2015. [Online]. [arXiv:1412.6980]
27. **Breiman L.** Random forests. *Machine Learning* 45: 5–32, 2001. doi:10.1023/A:1010933404324.
28. **Pedregosa F, Varoquaux G, Gramfort A, Michel V, Thirion B, Grisel O, Blondel M, Prettenhofer P, Weiss R, Dubourg V, Vanderplas J, Passos A, Cournapeau D, Brucher M, Perrot M, Duchesnay E.** Scikit-learn: Machine Learning in Python. *J Mach Learn Res* 12: 2825–2830, 2011. <http://jmlr.org/papers/v12/pedregosa11a.html>
29. **McKinney W.** Data structures for statistical computing in Python. In: *Proceedings of the 9th Python in Science Conference*, 2010. doi:10.25080/Majora-92bf1922-00a.
30. **Oliphant TE.** *Guide to NumPy* (2nd ed.). North Charleston, SC: CreateSpace Independent Publishing Platform, 2015.
31. **Bland JM, Altman DG.** Statistical methods for assessing agreement between two methods of clinical measurement. *Lancet* 1: 307–310, 1986.
32. **Litton E, Morgan M.** The PiCCO monitor: a review. *Anaesth Intensive Care* 40: 393–409, 2012. doi:10.1177/0310057X1204000304.
33. **Cameron JD, Jennings GL, Dart AM.** Systemic arterial compliance is decreased in newly-diagnosed patients with coronary heart disease: implications for prediction of risk. *J Cardiovasc Risk* 3: 495–500, 1996.
34. **Stergiopoulos N, Westerhof N.** Determinants of pulse pressure. *Hypertension* 32: 556–559, 1998. doi:10.1161/01.hyp.32.3.556.
35. **Haluska BA, Matthys K, Fathi R, Rozis E, Carlier SG, Marwick TH.** Influence of arterial compliance on presence and extent of ischaemia during stress echocardiography. *Heart* 92: 40–43, 2006. doi:10.1136/hrt.2004.052209.
36. **Bruinsma P, Arts T, Dankelman J, Spaan JAE.** Model of the coronary circulation based on pressure dependence of coronary resistance and compliance. *Basic Res Cardiol* 83: 510–524, 1988. doi:10.1007/BF01906680.
37. **Mitchell GF.** Arterial stiffness and hypertension: chicken or egg? *Hypertension* 64: 210–214, 2014. doi:10.1161/HYPERTENSIONAHA.114.03449.
38. **Chirinos JA, Segers P, Hughes T, Townsend R.** Large-artery stiffness in health and disease. *J Am Coll Cardiol* 74: 1237–1263, 2019. doi:10.1016/j.jacc.2019.07.012.